COBEM 2023 27TH INTERNATIONAL CONGRESS OF MECHANICAL ENGENEERING

ABCM Brazilian Society of Mechanical Sciences and Engineering
27th ABCM International Congress of Mechanical Engineering
December 04-08, 2023, Florianópolis-SC, Brazil

COB-2023-0666
A COMPARATIVE NUMERICAL ANALYSIS OF VENTURIMETER DESIGN STANDARDS APPLIED TO THE OPTIMIZATION OF FORMULA SAE RESTRICTOR

Juan Denner Campos da Silva [1]
Juan Carlos Assis Silva[2]
Rômulo Bessi Freitas[1,2]
Vinicius Ribeiro dos Santos de Sá Brito[1]
Paulo Roberto Farias Junior[1,2]
[1]Centro Federal de Educação Tecnológica Celso Suckow da Fonseca - CEFET-RJ - Nova Iguaçu
[2]Programa de Pós-Graduação em Engenharia Mecânica - Universidade Federal Fluminense
juan.campos@aluno.cefet-rj.br jcasilva@id.uff.br
romulo.freitas@cefet-rj.br
vinicius.brito@cefet-rj.br
paulo.farias@cefet-rj.br

Abstract. *Formula SAE is an important university competition, where a formula style racecar must be entirely designed and built by students. The air intake in the engine is a crucial part of the project since the competition requires the inclusion of a restrictor. Two standards for the venturimeter can be found, ISO 5167-4:2003 and ASME PTC 19.5-2004. However, there are divergences regarding the dimensions of the venturi's throat. The present analysis aims to evaluate each geometry, in order to assist in choosing the standard. Numerical simulations are performed using the open source code OpenFOAM to solve the two-dimensional incompressible Reynolds averaged Navier-Stokes equations. The results suggest that the lower throat ratio geometries produce greater mass flow.*

Keywords: *Venturimeter, Restrictor Standard, Formula SAE, ISO 5167-4:2003, ASME PTC 19.5-2004.*

1. INTRODUCTION

Formula SAE is a university competition organized by the Society of Automotive Engineers (SAE). Its purpose is to provide undergraduate students with the experience of designing and building a Formula-type car. This competition offers a valuable opportunity for students to apply the theoretical concepts they have learned in engineering college. In Brazil, Formula SAE started in 2004, and since then, the number of participants has steadily grown year after year, with over 1,030 participants in 2018.

The "Formula SAE Rules" document presents the guidelines for the car's characteristics, encompassing all the regulations for the tournament. An important rule was introduced to ensure fairness among all teams and reduce the maximum power of the motor vehicle. This rule mandates the addition of an air restrictor to the intake manifold. The air admitted to the engine is forced to pass through a twenty-millimeter diameter orifice. If alternative geometries are used, the same area as the circular restrictor must be considered.

Imposing the restriction on the system can be achieved through various methods, and the choice of geometry plays a crucial role in determining the optimal conditions. The extensive literature on fluid mechanics reveals that the Bernoulli obstruction theory can be utilized to predict the flow behavior with a diameter restriction. In the context of a Formula-type racecar, the best conditions are those that minimize head losses, resulting in a smaller reduction in power. The Venturimeter geometry proves to be the superior option when compared to a Thin-Plate Orifice or Flow Nozzle (Cauchi *et al.*, 2006).

Several papers stand out among the multitude of published materials focusing on Venturimeter geometry for students interested in optimizing Formula SAE restrictors. Cauchi *et al.* (2006), using a 1D engine model, achieved a 40% increase in mass flow rate within certain pressure ratios. Baylar *et al.* (2009), employing the FLUENT software, successfully determined the mass injection rates for aeration applications.

Zhang (2017), utilizing FLUENT software, conducted an evaluation of the influence of several structural parameters on Venturi flow. The results indicated that the minimum pressure occurs at the intersection between the contraction and the throat. Furthermore, the contraction ratio and the pressure difference between the inlet and outlet emerged as the primary geometry parameters affecting the velocity field.

Chen *et al.* (2014) and Kokkula *et al.* (2015) evaluated the influence of convergence and divergence angles in Venturi

flow, both employing FLUENT software. In their analyses, they did not consider the influence of the throat due to the absence of this geometry in their setups. More recently, Carrillo *et al.* (2018) used *OpenFoam* to compare experimental and numerical approaches, with results demonstrating good agreement and an error of less than 5%.

The Venturimeter construction standards provide two important references: ISO 5167-4:2003 and ASME PTC 19.5-2004. Although these standards present similar geometric features, a significant difference exists. ISO 5167-4:2003 specifies that the throat length must be equal to the throat diameter, while ASME PTC 19.5-2004 states that the throat length must be equal to the inlet diameter (Cauchi *et al.*, 2006). To support the choice of restrictor design, this paper aims to investigate the influences of throat ratio and divergence angle on the mass flux of Venturimeters applied in Formula SAE car intake systems.

2. METHODOLOGY

The methodology involved solving the Reynolds-Averaged Navier-Stokes equations using OpenFOAM, an open-source C++ library for Computational Fluid Dynamics (CFD). A finite volume scheme was utilized to discretize the computational domain, and a two-equation turbulence model based on the Boussinesq turbulent viscosity hypothesis was employed to close the turbulent stress terms. This approach allowed for the accurate prediction of flow behavior in the Venturimeter by capturing the mean effects of turbulence. The simulations facilitated the investigation of the influences of throat ratio and divergence angle on the mass flux, contributing to the optimization of Venturimeters in Formula SAE car intake systems.

2.1 Governing Equations

The governing equations for incompressible flow, known as the Navier-Stokes equations, are decomposed using the Reynolds decomposition $\phi = \overline{\phi} + \phi^{'}$, such that $\overline{\phi^{'}} = 0$, where the variables are split into mean and fluctuating components. The mean component, denoted by an overbar (e.g. $\overline{\phi}$), represents the time-averaged quantity, while the prime symbol (e.g. $\phi^{'}$) represents the fluctuating component. By applying this decomposition, the governing equations are modified to incorporate the temporal averaging of the pressure and velocity vector. The resulting equations are:

$$\frac{\partial \overline{u}_j}{\partial x_j} = 0 \tag{1}$$

$$\frac{\partial}{\partial x_j}(\overline{\rho} \overline{u}_i \overline{u}_j + \overline{p}\delta_{ij} - \tau_{ij} - \tau_{ij}^t) = 0 \tag{2}$$

where u_j is the velocity vector, p is the pressure, δ_{ij} is the Kronecker delta, τ_{ij} is the viscosity stress tensor and τ_{ij}^t is the Boussinesq-Reynolds tensor.

The system of equations (1) - (2) is underdetermined as it contains more variables than equations. To close the system, a turbulence model is employed, which provides additional equations. In this study, the $k - \varepsilon$ model was utilized to solve the Reynolds-Averaged Navier-Stokes (RANS) equations. The $k - \varepsilon$ model equations are given by:

$$\frac{\partial}{\partial x_j}(\rho k \overline{u}_i) = \frac{\partial}{\partial x_j}[(\mu + \frac{\mu_t}{\sigma_k})\frac{\partial k}{\partial x_j}] + P_k + P_b - \rho\varepsilon - Y_m \tag{3}$$

$$\frac{\partial}{\partial x_j}(\rho \varepsilon \overline{u}_i) = \frac{\partial}{\partial x_j}[(\mu + \frac{\mu_t}{\sigma_\varepsilon})\frac{\partial \varepsilon}{\partial x_j}] + C_{1\varepsilon}\frac{\varepsilon}{k}(P_k + C_{3\varepsilon}P_b) - C_{2\varepsilon}\rho\frac{\varepsilon^2}{k'} \tag{4}$$

where k is the turbulent kinetic energy $(\overline{u'u'}/2)$, ε is the dissipation energy and the turbulent kinematics viscosity is given by

$$\mu_t = \rho c_\mu \frac{k^2}{\varepsilon} C_\mu = 0.09 \tag{5}$$

The constants are adjusted semi-empirically and can be show in (Freitas, 2012). In the viscous sublayer a wall law is enforced.

2.2 Computational Domain

The computational domain was designed based on the intake system of the Fiúsa-019, a car from the Satirus team at CEFET/RJ. Figure (1c) illustrates the Venturimeter integrated into the Fiúsa-019 intake system, while Figure (1a) presents a schematic drawing of the Venturi tube with the adopted nomenclature. Four configurations were compared to investigate the influence of the throat ratio (TR = b/d), which represents the ratio between the length and diameter of the throat. The

chosen geometric parameters followed the recommendations of ASME PTC 19.5-2004, with TR = 1.9, and ISO 5167-4:2003, with TR = 1. The inlet and outlet diameters were determined based on fixed project conditions. The convergence angle was set at 21° (2α = 21°) for both standards, and the divergence angles used ranged between the upper and lower limits suggested by the standards (2β = 7° and 2β = 15°).

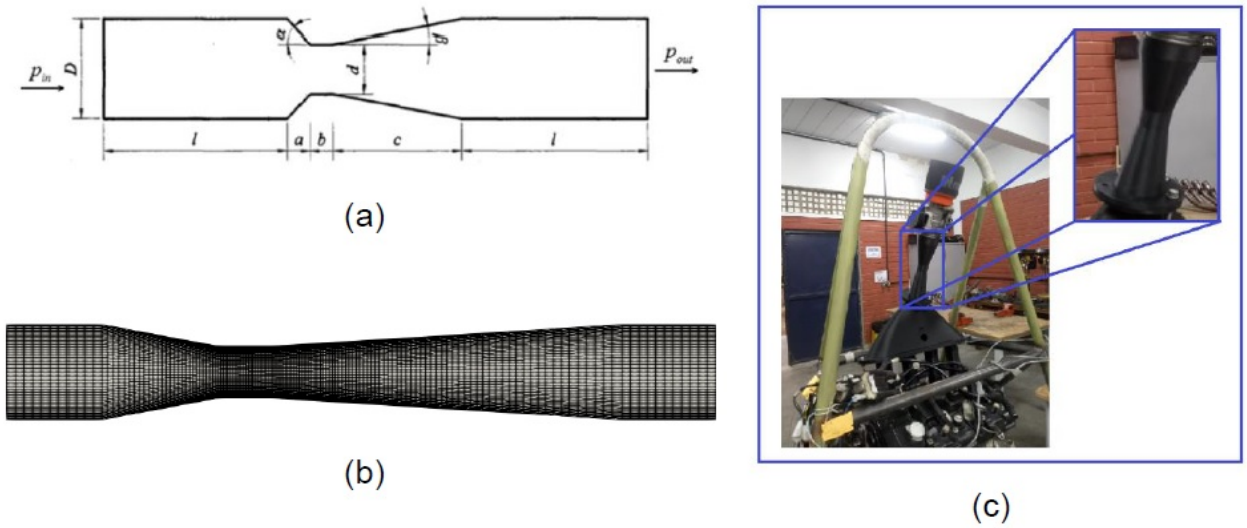

Figure 1. Computational Domain: (a) Geometric parameters for venturimeter. (b) 2D mesh using blockMesh library. (c)Venturimeter coupled in the admission of the Fiúsa-019, Satirus SAE car.

A two-dimensional computational mesh was generated using the blockMesh library in OpenFOAM. Grid refinement was focused on the walls and the throat region to ensure accuracy in those regions. Figure (1b) provides an example of these refined meshes. The inlet and outlet lengths were set equal to the diameter (D) since these parameters do not significantly influence the Venturi simulations, as demonstrated by Araoye *et al.* (2017).

2.3 Numerical Method

The governing equations are numerically solved using an unstructured finite volume scheme implemented in the open-source software OpenFOAM. The solution approach is based on a segregated, incompressible version of the pressure-based SIMPLE algorithm, employing a steady-state solver. An algebraic multigrid solver is utilized for the pressure equation, while a smooth solver is employed for the turbulent quantities and velocity equation, utilizing a Gauss-Seidel method. The vector field is interpolated using a Gauss linear scheme or a combination of Gauss linear scheme and first-order Gauss upwind scheme to ensure accurate and stable results.

2.4 Boundary Condition

The boundary conditions for the simulations are as follows: at the inlet, a total pressure of p0 = 101325 Pa is imposed, while at the exit, the pressure is defined. Five different exit pressure values (p) are considered, corresponding to pressure ratios (PR) of 1.002, 1.004, 1.006, 1.008, and 1.01. The initial field is specified by the inlet pressure, and the velocity field is set to zero. For solid boundaries, a no-slip condition is enforced for the velocity components.

In turbulent flows, the initial and boundary values for the turbulence quantities play a crucial role. The kinetic energy and dissipation rate (ϵ) can be calculated based on the given turbulent intensity (I), turbulent length scale (L), and the ratio of turbulent viscosity to molecular viscosity (μ_t/μ). These values are important for accurately simulating turbulent flows.

$$K = \frac{3}{2}(\overline{u}I)^2 \tag{6}$$

$$I = \frac{u^{'}}{\overline{u}} \tag{7}$$

$$\epsilon = C_\mu \frac{k^{3/2}}{L} \tag{8}$$

where C_μ a fitting constant and the length scale is given as a percentage of the characteristic length of the problem. The turbulent intensity used for all present cases are equal to 5% and the characteristic length scale is the diameter of throat.

2.5 Grid Refinement Study and Residue Control

To ensure grid independence, a grid refinement study was conducted. The mass flux was selected as the control parameter to determine the optimal number of cells in the mesh. Figure 2 (A) illustrates the mass flux for the flow through the venturimeter at a pressure ratio (PR) of 1.01, using five different mesh sizes. The results indicate that there is no significant change in the results, with variations of less than 1%. Based on this analysis, all subsequent computations were performed using a mesh consisting of 9250 cells.

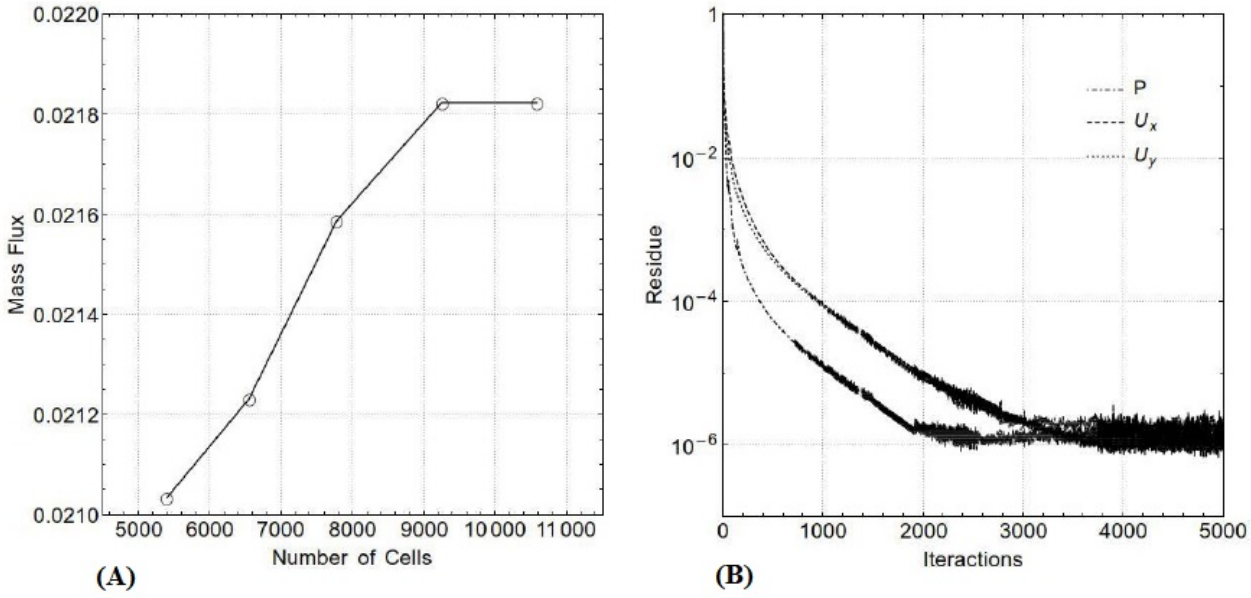

Figure 2. (A) - Mesh refinement study and (B) - Residue control

The numeric residue was controlled to all simulations, given the accuracy with six digits of precision. Figure 2 (B) shows the rate of residue decay as a function of the number of interations. Usually, the residue reaches the digits of precision with 3000 iterations, however the maximum ones was set to 5000.

3. RESULTS AND DISCUSSION

The computational model and boundary conditions were initially validated by comparing preliminary results with analytical equations. The theoretical results were obtained using the Bernoulli equation combined with the mass conservation law, with the velocity at the venturimeter throat serving as the parameter for comparison. Figure (3) demonstrates the good agreement between the numerical and theoretical results, with a maximum relative error of 6%. This validation confirms the accuracy of the computational model in capturing the flow behavior in the venturimeter.

To investigate the influence of the throat ratio, a total of five simulations were conducted for each studied geometry, with varying boundary pressure conditions. The simulations were carried out under the operating condition of the SAE car engine, which operates at 7000 RPM (revolutions per minute). The corresponding theoretical mass flux at the engine is $0.0379\,kg/s$, resulting in a maximum velocity at the throat of 126 m/s. Considering this operating condition, the pressure ratio (PR) was imposed as PR = pin/pout = 1.002, 1.004, 1.006, 1.008, and 1.01. These different pressure ratios allowed for the investigation of the flow behavior and performance of the venturimeter across a range of operating conditions.

The mass flux was calculated for all studied geometries according to the curves in Figure (4), and the results are presented in Figure (5). The throat with a ratio of TR = 1.0 proved to be the optimal choice, as it exhibited the highest mass flux. The maximum mass flux was achieved when TR = 1.0 and $\phi = 15^0$, resulting in a significant gain of 15.8% for PR = 1.01. It is observed that there is a direct relationship between performance and the minimum pressure at the throat. Specifically, a lower pressure at the throat leads to a higher mass flow. This finding aligns with the results obtained by Zhang (2017), further validating the observations made in this study.

However, it was expected that increasing the divergence angle would lead to a decrease in the mass flux due to the formation of recirculation bubbles. Surprisingly, this phenomenon did not occur under the operating conditions studied. The absence of recirculation zones for the considered divergence angles can be attributed to the specific operating conditions. Therefore, the difference in mass flux can be attributed to friction losses along the venturi length. Higher divergence angles allow for shorter venturi lengths, reducing these losses. However, it is important to note that this effect does not

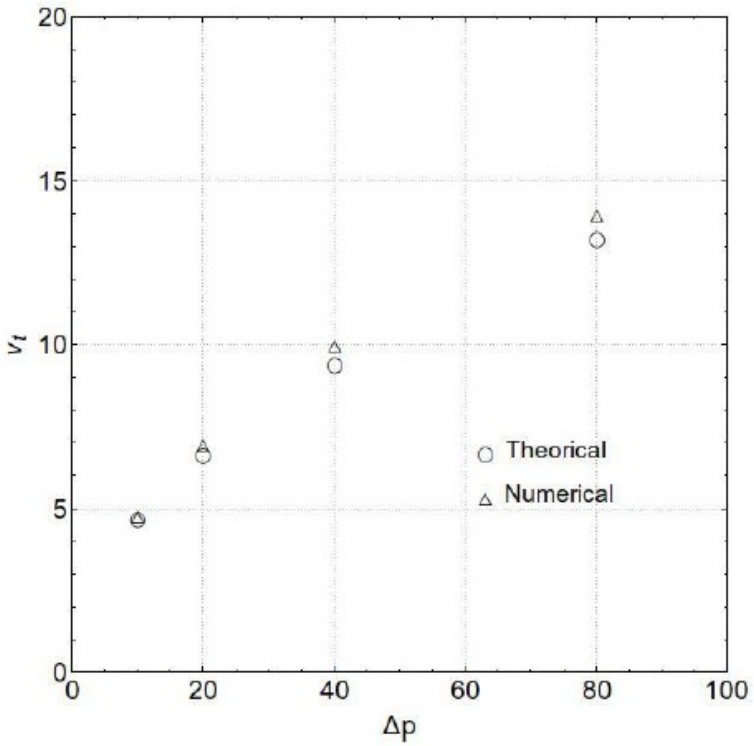

Figure 3. Velocity in venturimeter throat x differential pressure

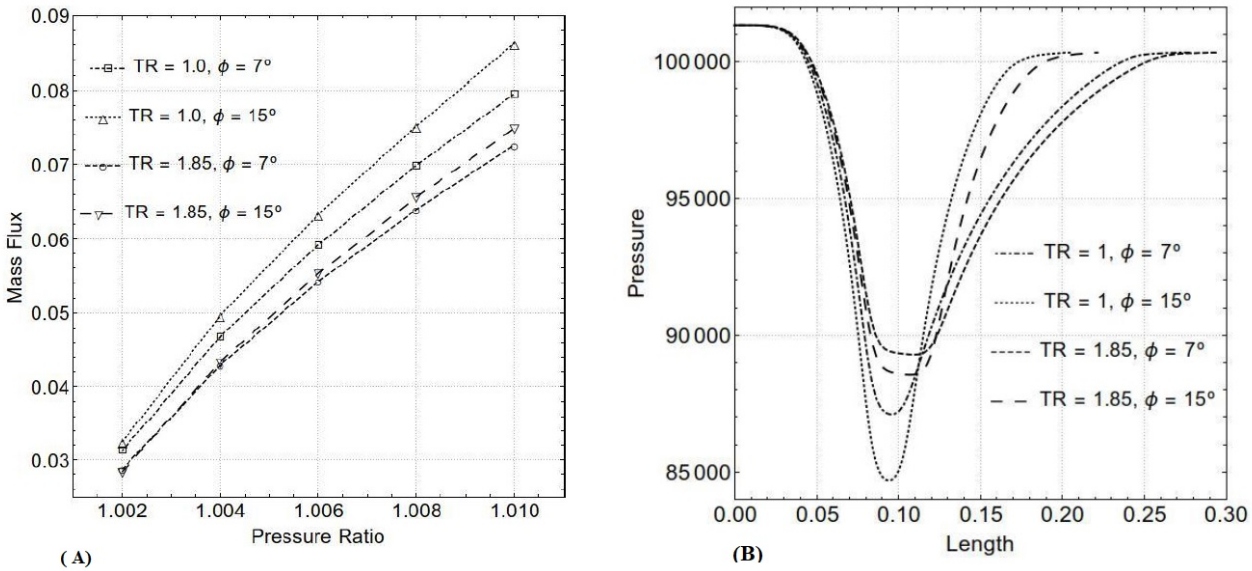

Figure 4. (A) - Mass flux vs Pressure ratio (B) - Pressure vs Venturi length

occur when the divergence angle is sufficiently high, resulting in the generation of recirculation zones in the divergence zone.

4. CONCLUSIONS

The ISO 5167-4:2003 and ASME PTC 19.5-2004 standards were evaluated to determine their effectiveness in designing the restrictor for Formula SAE applications. The OpenFOAM software was utilized to calculate the mass flow through the Venturimeter. Throat ratios of TR = 1 and TR = 1.9 were considered, based on the recommendations of each standard. Under the operating conditions of a Formula SAE car, it was observed that TR = 1 exhibited the best performance for the air intake system. This indicates that the ISO 5167-4:2003 standard should be adopted for restrictor design. The findings of this study provide valuable insights for optimizing the performance of Venturimeters in Formula SAE car intake systems.

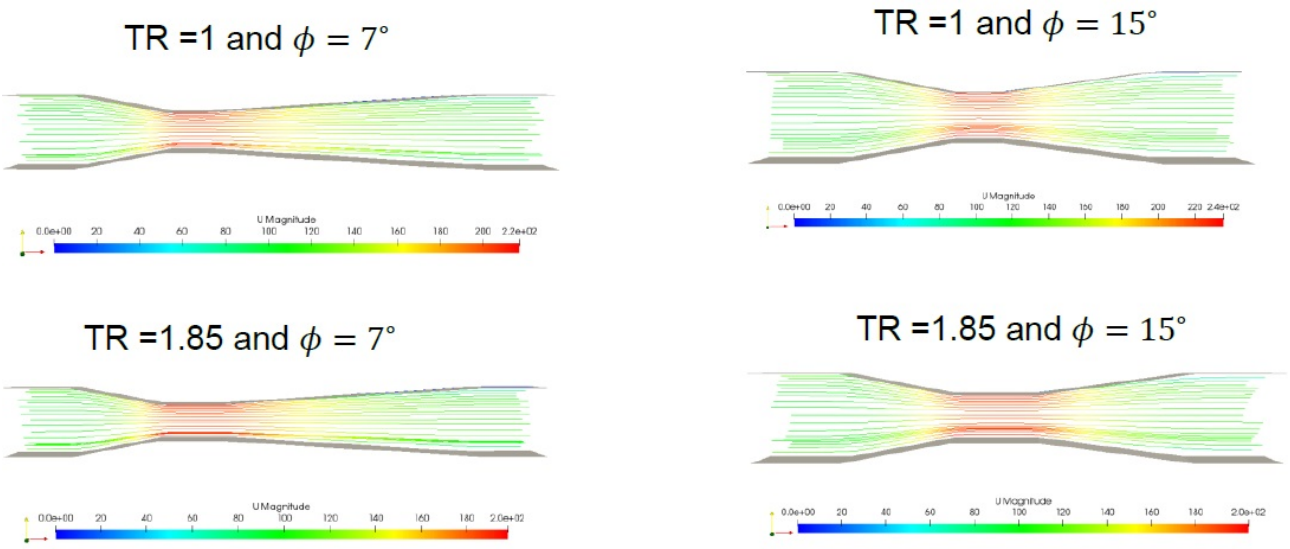

Figure 5. Streamlines velocity through venturimeter with PR = 1.01.

Furthermore, from the analysis of the streamlines, it was observed that no recirculation bubbles were formed for the divergence angles investigated. The results indicated that larger divergence angles resulted in higher mass flow rates. Therefore, the geometry with a throat ratio of TR = 1 and a divergence angle of $2\beta = 15^0$ demonstrated the best performance among those evaluated in this study. However, it is important to note that there is a maximum divergence angle that should be considered when designing the restrictor. Going beyond this maximum angle may lead to adverse effects on the flow behavior and performance of the Venturimeter. Hence, careful attention must be given to choosing an appropriate divergence angle during the restrictor design process.

5. ACKNOWLEDGMENTS

The authors would like to thank CEFET/RJ - UNED Nova Iguaçu for their support and resources. Special thanks to FAPERJ for funding this project (E-26/010.000864/2019). The authors also acknowledge the valuable contribution of COMPRINT Company for their expertise in 3D printing. Lastly, heartfelt appreciation goes to the SATIRUS FSAE team for their collaboration in advancing engineering knowledge. JCAS would like to thank FAPERJ for Mestrado Nota 10 scholarship.

6. REFERENCES

Araoye, A.A., Badr, H.M. and Ahmed, W.H., 2017. "Investigation of flow through multi-stage restricting orifices". *Annals of Nuclear Energy*, Vol. 104, pp. 75–90.

Baylar, A., Aydin, M.C., Unsal, M. and Ozkan, F., 2009. "Numerical modeling of venturi flows for determining air injection rates using fluent v6. 2". *Mathematical and Computational Applications*, Vol. 14, No. 2, pp. 97–108.

Carrillo, V., Jerves, R., Lucero, F. *et al.*, 2018. "Experimental and numerical simulation as a calibration measure of a venturi tube". *International Journal of Hydrology*, Vol. 2, No. 2.

Cauchi, J., Farrugia, M. and Balzan, N., 2006. "Engine simulation of a restricted fsae engine, focusing on restrictor modelling". Technical report, SAE Technical Paper.

Chen, C.W., Du, W., Sun, J.Q., Liu, W., Chang, Y. and Dong, W., 2014. "Simulation analysis and design of intake restrictor of fsae race car". *Applied Mechanics and Materials*, Vol. 602, pp. 751–756.

Freitas, L., 2012. *Simulação numérica de perdas em selo do tipo labirinto com aplicação em turbinas a gás*. Master's thesis.

Kokkula, P.R., Bhojappa, S., Arslan, S. and Jawad, B.A., 2015. "Design and optimization of the restrictor of a race car". In *ASME International Mechanical Engineering Congress and Exposition*. American Society of Mechanical Engineers, Vol. 57472, p. V07BT09A038.

Zhang, J., 2017. "Analysis on the effect of venturi tube structural parameters on fluid flow". *AIP Advances*, Vol. 7, No. 6.

7. RESPONSIBILITY NOTICE

The authors are solely responsible for the printed material included in this paper.